atmosphere

MDPI

Supporting Information for

Spring 2018 Asian dust events: Sources, Transportation, and Potential Biogeochemical Implications

Joo-Eun Yoon [1], Jae-Hyun Lim [2], Jeong-Min Shim [2], Jae-Il Kwon [3], and Il-Nam Kim [1,*]

[1] Department of Marine Science, Incheon National University, Incheon 22012, Republic of Korea; jeyoon@inu.ac.kr (J.E.Y.)

[2] Fisheries Resources and Environment Division, East Sea Fisheries Research Institute, National Institute of Fisheries Science, Gangneung 25435, Republic of Korea; lim900@korea.kr (J.H.L.); jmshim67@korea.kr (J.M.S.)

[3] Marine Disaster Research Center, Korea Institute of Ocean Science & Technology, Busan, Republic of Korea; jikwon@kiost.ac.kr

* Correspondence: ilnamkim@inu.ac.kr; Tel.: +82-32-835-8864

Text S1. The influence of cloud interferences on AI estimates.

Figure S1 showed that dust storms occurred during 26 March to 4 April were influenced by cloud interferences. Thus, to investigate the uncertainty in the AI estimates from the S-NPP OMPS observations given the cloud conditions, we have compared AI values estimated from the cloud-free areas (green boxes shown in Figure S1) vs. the cloud-covered areas (blue boxes shown in Figure S1) along dust pathways (Figures 2 and S2). The AI difference ranged from 0.2 to 0.4 (Table S1), indicating that cloud interferences were not significant during the study period.

Table 1. Comparison of AI values for green boxes (cloud-free condition) and blue boxes (cloud-covered condition) shown in Figure S1.

	Cloud-free condition		Cloud-covered condition	
	Area	**AI value**	**Area**	**AI value**
26 March	43–45° N, 105–107° E	1.7	42–44° N, 120–122° E	1.4
28 March	44–46° N, 137–139° E	2.8	47–49° N, 140–142° E	2.6
29 March	37–39° N, 122–124° E	3.9	35–37° N, 124–126° E	3.5
02 April	47–49° N, 133–135° E	2.8	45–47° N, 131–133° E	2.4
03 April	38–40° N, 134–136° E	1.5	40–42° N, 138–140° E	1.8

Table 2. OPP (mg C m^{-2} d^{-1}) and OEP (mg C m^{-2} d^{-1}) estimates averaged over a 13-day period (17–29 April) in 2018 and mean values averaged over the same period between 2012 and 2017. Data were averaged for the dust-affected area (cyan square) shown in Figure 7c.

	2018	**Mean (2012–2017)**	**Ref.**
OPP	381.1 ± 151.4	257.9 ± 29.5	
OEP (Dunne07 model)	163.7 ± 86.2	79.0 ± 11.1	[1]
OEP (Laws11 model)	88.4 ± 46.2	51.0 ± 7.2	[2]

OEP (Henson11 model)	77.0 ± 29.0	51.4 ± 4.5	[3]

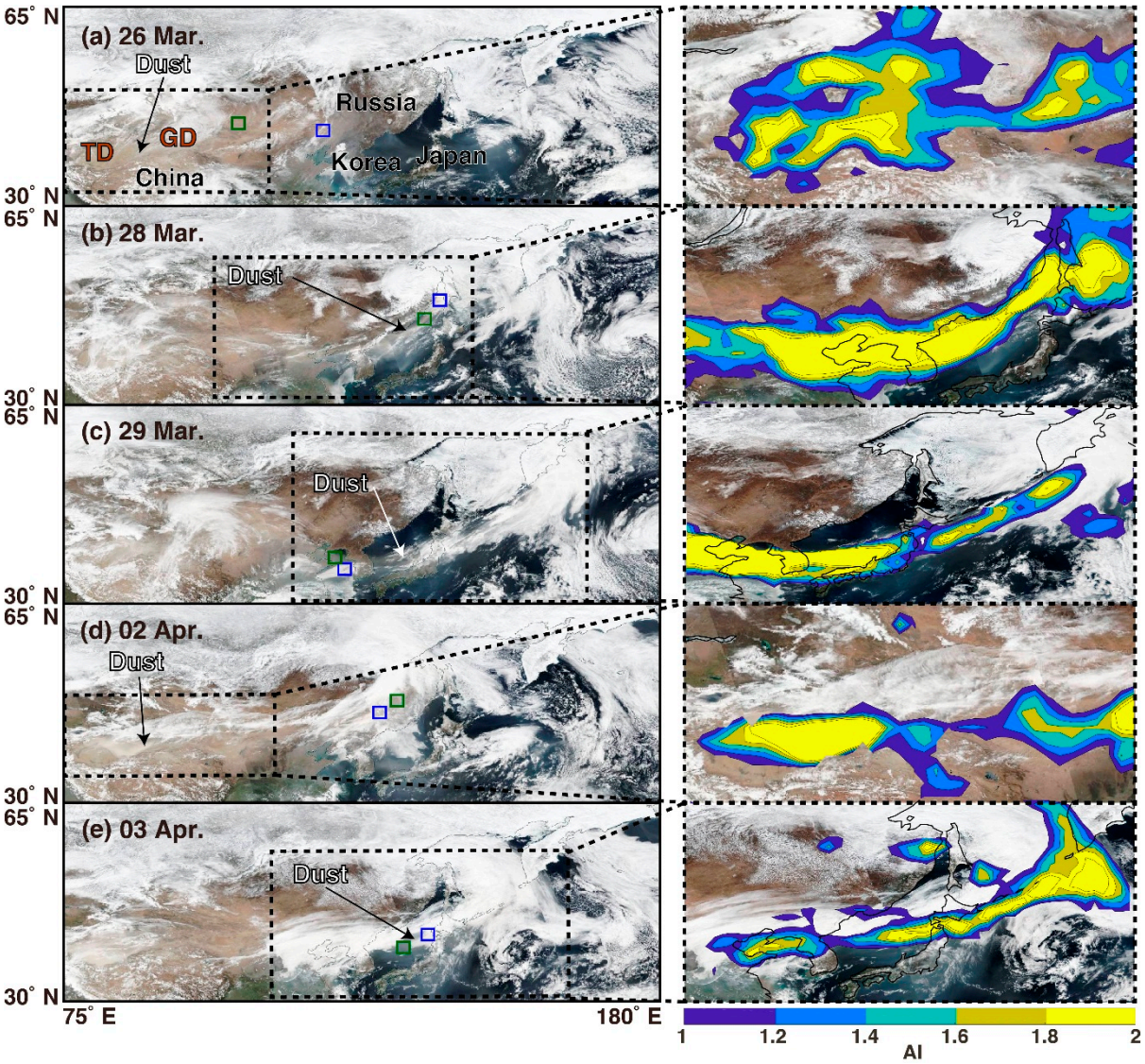

Figure 1. (a–e) The S-NPP VIIRS true color images for 26, 28–29 March and 2–3 April, 2018. Black dotted box indicates the dust outbreak and transport recognized as a yellow-brownish color and it was overlaid with the AI values as contour lines. TD is the Taklimakan desert and GD is the Gobi desert. Green boxes indicate cloud-free conditions and blue boxes indicate cloud-covered conditions.

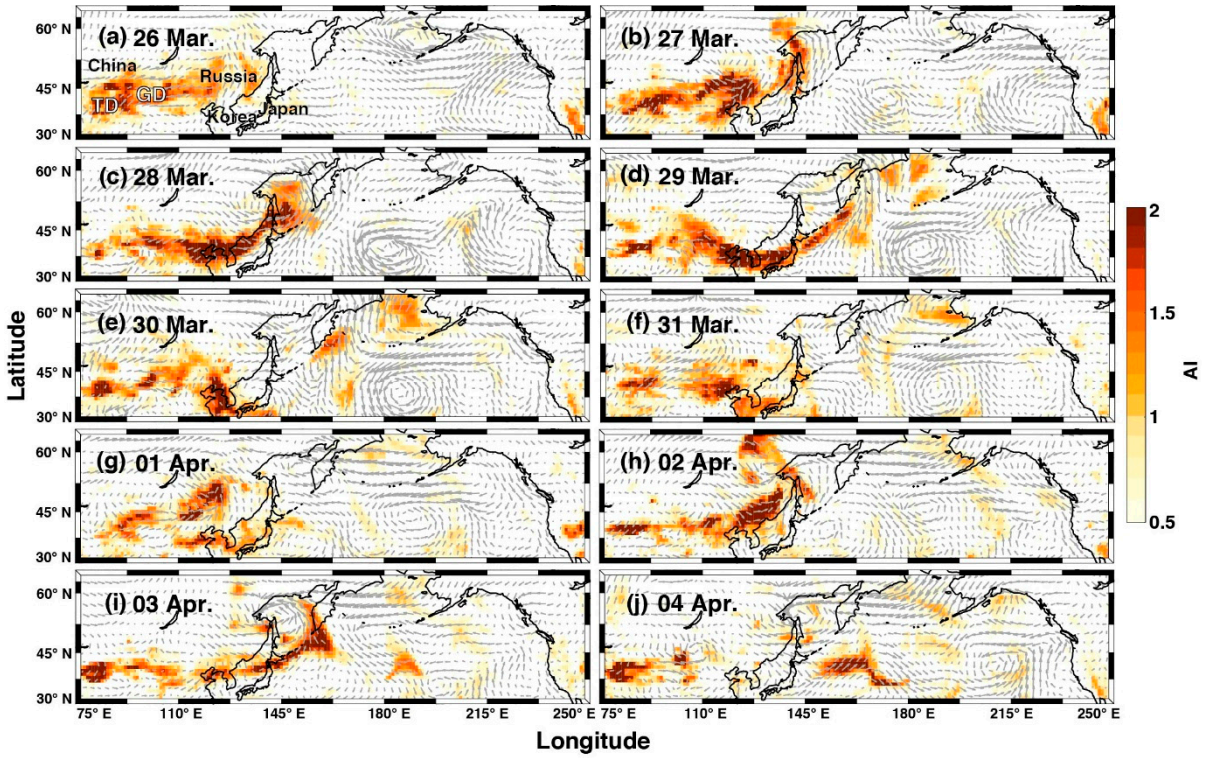

Figure 2. (a–j) Spatial distributions of AI from 26 March to 04 April, 2018. The grey arrows represent daily surface wind vectors.

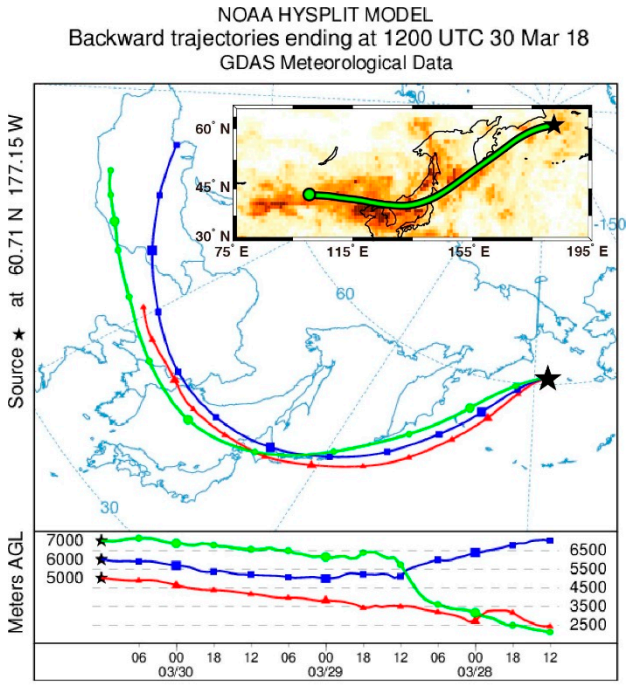

Figure 3. Back trajectories derived from the NOAA HYSPLIT model at different altitude levels (5000, 6000, 7000 m; red line, blue line, green line, respectively) in Bering Sea (black star; 60.71° N, 177.15° W) on 12:00 UTC 30 March, 2018. The inset figure indicates the back trajectory at 7000 m overlaid onto Figure 3a.

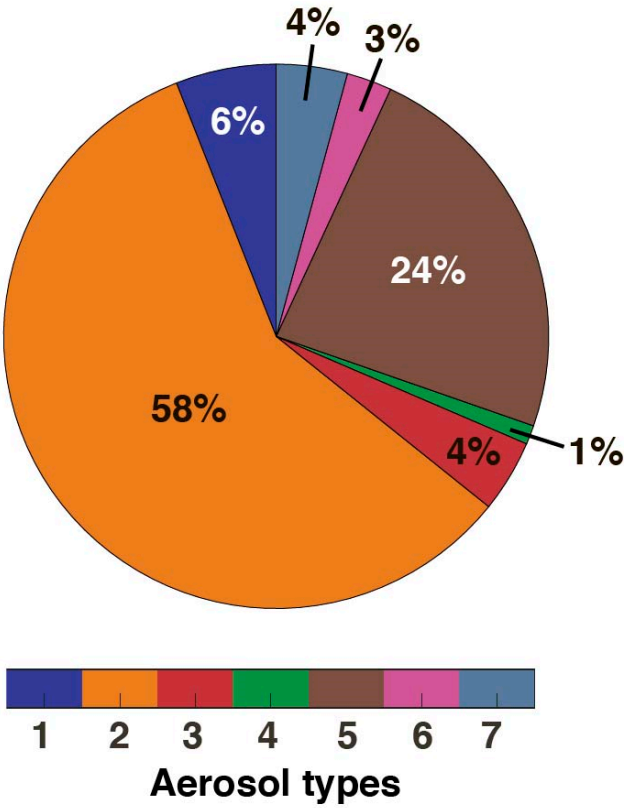

Figure 4. Pie chart of the mean composition of aerosols types along orbit paths shown in Figure 5a. Colorbar indicates aerosol types defined as clean marine (1), mineral dust (2), polluted continental/smoke (3), clean continental (4), polluted dust (5), elevated smoke (6), and dusty marine (7).

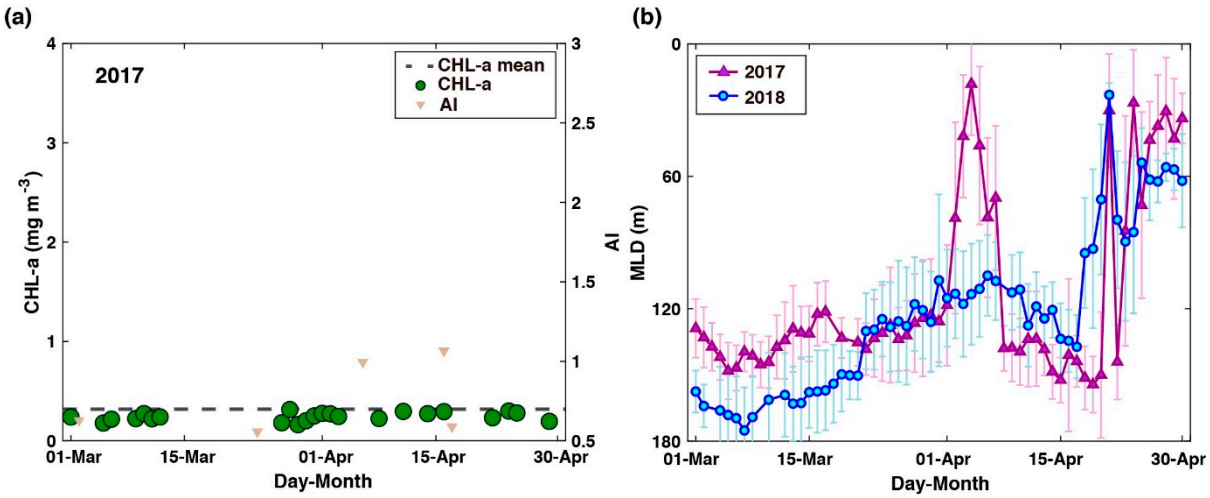

Figure 5. (a) Daily AI values (triangles) and daily CHL-a concentrations (mg m^{-3}, circles) during the 2017 spring for the area marked as a cyan square in Figure 7c. The black dotted line indicates mean CHL-a concentrations averaged for values from March to April in 2012–2017. (b) Daily MLD during the 2017/2018 spring in cyan square in Figure 7c.

References

1. Dunne, J.P.; Sarmiento, J.L.; Gnanadesikan, A. A synthesis of global particle export from the surface ocean and cycling through the ocean interior and on the seafloor. *Global Biogeochem. Cycles* **2007**, *21*.
2. Laws, E.A.; D'Sa, E.; Naik, P. Simple equations to estimate ratios of new or export production to total production from satellite-derived estimates of sea surface temperature and primary production. *Limnol.*

Oceanogr. **2011**, *9*, 593-601.
3. Henson, S.A.; Sanders, R.; Madsen, E.; Morris, P.J.; Le Moigne, F.; Quartly, G.D. A reduced estimate of the strength of the ocean's biological carbon pump. *Geophys. Res. Lett.* **2011**, *38*, L04606.